Available online at www.sciencedirect.com

ScienceDirect

Energy Procedia 38 (2013) 108 – 113

Energy Procedia

SiliconPV: March 25-27, 2013, Hamelin, Germany

Weak light performance of PERC, PERT and standard industrial solar cells

Jan Krügener[a,]* and Nils-Peter Harder[a,b]

[a]Insitute of Electronic Materials and Devices (MBE), Schneiderberg 32, 30167 Hannover, Germany
[b]Institute for Solar Energy Research Hamelin (ISFH), Am Ohrberg 1, 31860 Emmerthal, Germany

Abstract

We use SENTAURUS DEVICE simulation to investigate the effect of "passivated emitter and rear cell" (PERC) and "passivated emitter and rear, totally-diffused" (PERT) device architecture on the solar cells' weak light performances. Injection-dependent carrier lifetimes can also strongly influence the fill factor and weak light performance of solar cells. To focus on the effect of the device architecture alone, we present here simulations with essentially injection independent carrier lifetimes. In our simulations we find that at 1/10 of AM1.5G ("tenth of one sun") the standard industrial cell architecture with full-area BSF loses about 1.7 % efficiency and the similar PERT cell structure loses 1.4 % to 1.6 %, depending on wafer quality. The PERC cells suffer only 1.2 % to 1.5 % loss of efficiency at 1/10 sun. The lower losses for PERC solar cells result from the fact that at lower illumination intensity the relatively high resistance of PERC cells is less significant. We furthermore find that only for PERC solar cells the optimum wafer doping concentration depends on the illumination intensity.

Keywords: Simulation; PERC; PERT; weak light

1. Introduction

Standard solar cells are typically characterized under illumination of "1-Sun" (AM1.5G), although in regions where the AM1.5G spectrum is supposed to be the standard illumination - such as central Europe - most of the times solar modules in the field operate under much lower light intensity. Here we present SENTAURUS DEVICE simulation results about the influence of weak light conditions on the

* Corresponding author. Tel.: +49 (0)511-762-5009; fax: +49 (0)511-762-4229
E-mail address: kruegener@mbe.uni-hannover.de

doi:10.1016/j.egypro.2013.07.256

performance of standard industrial cells in comparison to "passivated emitter and rear cell" (PERC) [1-6] and "passivated emitter and rear, totally-diffused" (PERT) [7,8] solar cells. In our study we simulate all of these solar cell structures for p-type material to focus on the effect of the device architecture. In industrial application, PERT solar cells are primarily investigated for n-type wafers [9-12] in order to avoid the recombination from boron-oxygen-complexes.

We simulate the performance for wafer resistivities in the range from 0.04 Ωcm to 1300 Ωcm for high- and low-quality wafers, respectively, including boron-oxygen-related recombination. All diffused layers were modelled with a sheet resistance of 80 Ω/sq. Our simulations show efficiencies between 20 % and 20.9 %. We find peak efficiencies of 20 % (standard cell), 20.6 % (PERC) and 20.9 % (PERT) under AM1.5G together with the same generation profile for all structures. Assuming the same generation profile slightly favours the standard cell design compared to the more advanced rear passivated PERC and PERT cells. At 1/10 intensity the standard cell loses ~1.7% efficiency, the PERT cell loses 1.4% to 1.6%, depending on wafer quality, and the PERC cell 1.2% to 1.5% (same generation profile for all structures).

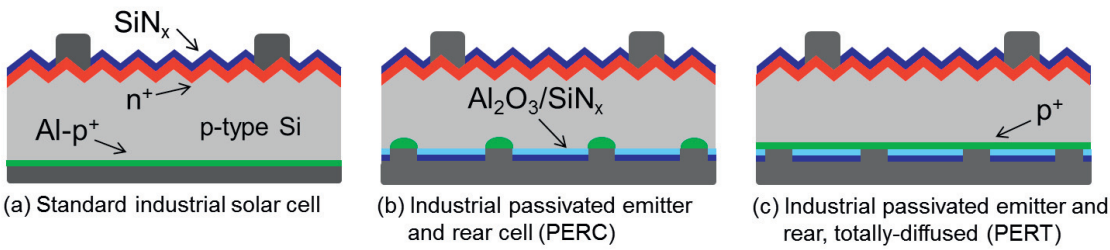

Fig. 1. - Geometric models of (a) standard industrial, (b) PERC and (c) PERT solar cells as used for the simulations.

2. Model

In 2-dimensional numerical simulations using SENTAURUS DEVICE, we calculate the current-voltage (*IV*) characteristics of standard industrial solar cells and of advanced PERC and PERT solar cells and determine the typical performance parameters such as efficiency, open circuit voltage, short circuit current, fill factor and series resistance as a function of the base doping concentration. We compare the weak light performance of these cell designs in the resistivity range of 0.04 Ωcm to 1300 Ωcm.

In commonly used p-type Czochralski-grown silicon (Cz-Si), boron-oxygen-related recombination centres limit the bulk lifetime [13] and therefore the overall cell performance. Injection-dependent lifetime measurements show that the lifetime limiting boron-oxygen-related recombination centre can be described by one midgap (0.41 eV below conduction band) centre after Shockley-Read-Hall (SRH). [14,15] For 0.4 ~ 10 Ωcm boron-doped p-type Cz-Si wafers, with a typical interstitial oxygen concentration of $[O_i] = 7.5 \cdot 10^{17}$ cm^{-3}, Schmidt *et al.* [16] provided a parameterization for the upper limit of experimentally observed carrier lifetimes. This parameterization relates to the cured state and is given by following formula [16]:

$$\tau_{n0} = 5.25 \cdot 10^{25} \cdot N_A^{-1.46} = 0.1 \cdot \tau_{p0} \qquad (1)$$

τ in µs and N_A in cm^{-3}. Without considering other recombination paths, this formula implies for lowly-doped material an unrealistically high SRH limit to the bulk lifetime, e.g. 191 ms for $N_A = 10^{14}$ cm^{-3}. In practice, not only Auger recombination and radiative recombination limit the bulk lifetime to much lower values, but also other additional SRH recombination via crystal defects and impurities. Therefore we include a "background" SRH recombination in our simulations in the following

manner: We introduce two cases where we limited the maximum SRH recombination parameters τ_n and τ_p to 200 µs ("low-quality material") and 10 ms ("high-quality material"), respectively. Fig. 2a shows the effective lifetime as a function of the excess carrier concentration including SRH recombination via boron-oxygen complexes. The shown SRH characteristic arises from equation 1 together with a base doping of $1 \cdot 10^{15}$ cm^{-3}. Injection-dependent carrier lifetimes, such as also observable in Fig. 2a, can strongly influence the fill factor and weak light performance of solar cells. This injection dependency is actually a very important parameter for detailed studies in the low-level injection regime. In particular for low-quality material one often observes a decrease of the carrier lifetime towards low injections. This decrease is often found to extend much further [17] compared to the boron-oxygen recombination described by Bothe *et al*. [13]. However, this effect is very specific to the chosen material and depends on the extent of the "background" SRH recombination by extrinsic defects. In our study we want to focus on the effect of the device architecture alone. Therefore we model the "background" SRH recombination with no further injection dependence of the carrier lifetimes. The same injection independency was assumed for the surface recombination velocity. Thus, in addition to the SRH recombination induced by the boron-oxygen complexes, the "background" SRH recombination is modelled by $\tau_n = \tau_p$. We call the "background" SRH recombination with 200 µs = $\tau_n = \tau_p$ "low-quality material" and "background" SRH recombination with 10 ms = $\tau_n = \tau_p$ "high-quality material".

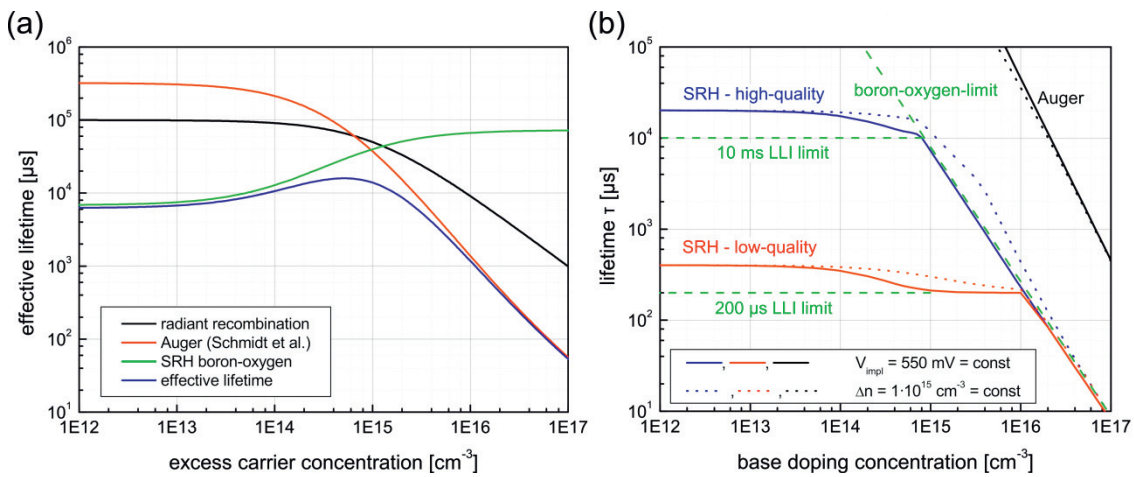

Fig. 2. (a) Effective lifetime as a function of the excess carrier density for boron-doped ($1 \cdot 15$ cm^{-3}) p-type silicon in the presence of SRH active boron-oxygen complexes; modelled after eq. (1). (b) SRH lifetime as a function of the base doping for high- (10 ms low-level injection limit) and low-quality (200 µs low-level injection limit) material. Lines correspond to lifetime for constant implied voltage (550 mV); dotted lines correspond to lifetime for a constant injection level of $1 \cdot 15$ cm^{-3}. Auger and boron-oxygen-limits are also shown.

In Fig. 2b the actually used lifetime as a function of the base doping concentration is plotted for high- (blue) and low-quality (red) material. Since all of the simulated solar cells operate at a maximum power point around 550 mV, the continuous lines provide the lifetimes for this operating voltage. For comparison, dotted lines are the lifetime at $\Delta n = 10^{15}$ cm^{-3}.

All cells investigated have an 80 Ω/sq n^+ emitter covered by a SiN_x layer and 70 µm wide metal fingers with an index of 2 mm. The rear of the standard industrial cells was modelled with a measured Al-BSF profile [18] and an adapted fix lifetime of 7 ns within the Al-BSF. The lifetime has to be adapted, to fit the experimentally observed value of 650 fA/cm² for the saturation current density. [19] For the PERC cells

we chose a rear side BSF line index of 1 mm. Local BSF lines have a shallower doping profile [20] and higher J_{0e} value compared to full-area BSF layers. We use 4 µm doping depth with a J_{0e} = 900 fA/cm². [21] The values of the contact resistivity (55 mΩ·cm²) at the local Al-BSF fingers were taken from references [22] and [23].

For the PERT cells we choose a 49 Ω/sq BSF and an index of 1 mm for the rear side contact fingers. The rear sides of the PERC and the PERT cells have a surface recombination according to a passivation by Al_2O_3/SiN_x stacks, which show very low surface recombination. [24,25] Note that the surface recombination velocity of Al_2O_3 passivation on p-type silicon is virtually injection independent and therefore typically does not cause significant loss of solar cell efficiency at low illumination intensities.

3. Results and discussion

Fig. 3 summarizes the results of the simulations for illuminations of "1-Sun" (filled symbols) and for "0.1-Sun" (open symbols). For each cell type (standard, PERC and PERT) and both illumination intensities the results for low-quality and high-quality material are shown.

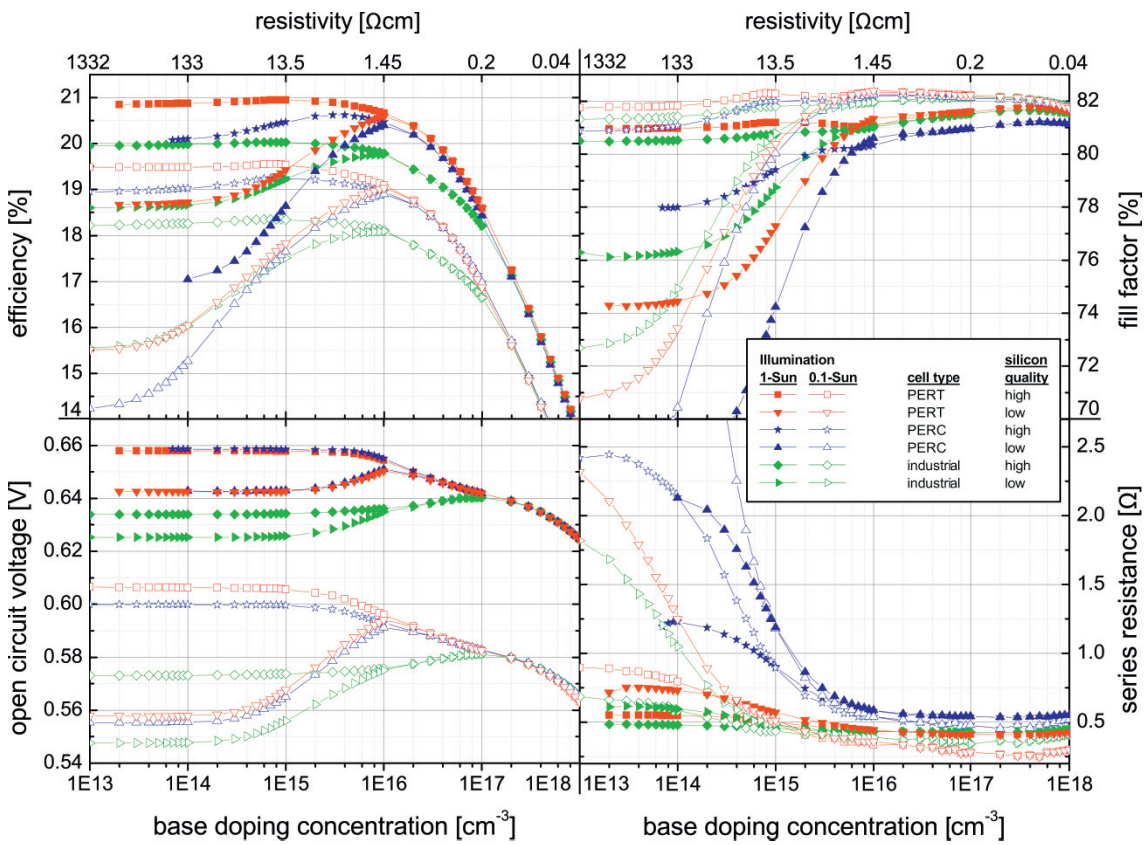

Fig. 3. Calculated cell efficiencies, fill factors, open-circuit voltages and series resistances as a function of the base doping concentration for different cell concepts. Full symbols correspond to the illumination of "1-Sun" (AM1.5G), open symbols correspond to "0.1-Sun". The same generation profile is assumed for all different cell structures.

The PERT solar cell shows the highest efficiencies (20.9 %), followed by the PERC cell (20.6 %) and the standard cell (20 %). We assumed the same generation profile for all cell structures. That slightly favours the standard cell, which usually suffers from the absence of a rear passivation.

However, the wafer doping dependence of both, the standard industrial cell with full-area Al-BSF and the PERT cell, show qualitatively very similar characteristics: For high-quality material both cell designs show highest efficiencies at very low base doping. Only for low-quality material a clear preference develops for doped wafers in standard cells and PERT cells, because the doping reduces the saturation current density (J_0) of the bulk and thus ensures high V_{OC} values.

For PERC solar cells, low wafer doping is not preferred. Even for high quality material the efficiency of PERC solar cells starts decreasing for wafer resistivities > 3 Ωcm, since the electrical resistance in the lowly-doped base limits the *FF* for these cells. When changing to low-quality material, the decrease of PERC cell efficiency towards high wafer resistivities becomes even more pronounced. In this case, the saturation current density contribution of the base volume becomes large, just as in the case of the standard and of the PERT cell. In addition, the *FF* limitations from the electrical transport through the high resistivity base are further amplified since the low-quality material makes the cell operate at lower voltages, which in turn leads to lower carrier densities in the bulk.

For all types of cells investigated here, at higher base doping (above 10^{16} cm^{-3}), the boron-oxygen-related SRH lifetime described with equation (1) becomes a limiting factor of the cells and reduces V_{oc}. In addition J_{sc} drops for base doping above 10^{16} cm^{-3} (not shown here).

Table 1. Change of cell efficiency in absolute percent between "1-Sun" (AM1.5G) and "0.1-Sun" illumination. Only in case of high-quality material in PERC cells the optimum wafer doping depends on illumination intensity. Case (a) refers to cells with doping optimized for "0.1-Sun" and (b) for "1-Sun".

	Δη: "1-Sun" → "0.1-Sun" for high-quality silicon	Δη: "1-Sun" → "0.1-Sun" for low-quality silicon
Standard cell	1.68 %	1.67 %
PERT	1.39 %	1.56 %
PERC	1.17 %[(a)] – 1.45 %[(b)]	1.50 %

Table I summarizes the change of cell efficiency between "1-Sun" and "0.1-Sun" illumination intensity. All cells operate less efficiently under "0.1-Sun" than under "1-Sun". The losses for PERC solar cells are smallest since the relatively high series resistance of PERC cells is less relevant at lower illumination intensity. In our simulations we find for almost all cases that the optimum wafer doping for the solar cells does not depend on the illumination intensity. Only for PERC solar cells made from high-quality material we find that the optimum doping concentration depends on the illumination intensity.

References

[1] A.W. Blakers, A. Wang, A.M. Milne, J. Zhao, and M.A. Green, "22.8 % efficient silicon solar cell", Appl. Phys. Lett. 55 (13), 1363-1365 (1989).

[2] A. Wang, J. Zhao, and M.A. Green, "24 % efficient silicon solar cells", Appl. Phys. Lett. 57 (6), 602-604 (1990).

[3] J. Schmidt, A. Merkle, R. Brendel, B. Hoex, M.C.M. van de Sanden, and W.M.M. Kessels, "Surface passivation of high-efficiency silicon solar cells by atomic-layer-deposited Al2O3", Prog. Photovolt: Res. Appl. 16 (6), 461-466 (2008).

[4] S. Gatz, H. Hannebauer, R. Hesse, F. Werner, A. Schmidt, T. Dullweber et al., "19.4 %-efficient large-area fully screen-printed silicon solar cells", physica status solidi RRL 5 (4), 147-149 (2011).

[5] S. Mack, U. Jäger, G. Kästner, E.A. Wotke, U. Belledin, A. Wolf et al., "Towards 19 % efficient industrial PERC devices using simultaneous front emitter and rear surface passivation by thermal oxidation", Proceedings of the 35th IEEE Photovoltaic Specialists Conference (PVSC) 2010, Honolulu, USA, 2010.

[6] T. Böscke, R. Hellriegel, T. Wütherich, L. Bornschein, A. Helbig, R. Carl et al., "Fully Screen-Printed PERC cells with Laser-Fired Contacts – An Industrial Cell Concept with 19.5 % Efficiency", Proceedings of the 37th IEEE Photovoltaics Specialists Conference, 003663-003666, Seattle, Wash, USA, 2011.

[7] J. Zhao, A. Wang, and M.A. Green, "24.5 % Efficiency Silicon PERT Cells on MCZ Substrates and 24.7 % Efficiency PERL Cells on FZ Substrates", Prog. Photovolt: Res. Appl. 7, 471-474 (1999).

[8] J. Zhao, A. Wang, P.P. Altermatt, M.A. Green, J.-P.P. Rakotoniaina, O. Breitenstein, "High Efficiency PERT cells on n-Type Silicon Substrates", 29th IEEE Photovoltaics Specialists Conference, 218-221, Sydney, Australia, 2002.

[9] A. Weeber, R. Naber, N. Guillevin, P. Barton, A. Carr, D. Saynova et al., "Status of n-Type Solar Cells for Low-Cost Industrial Production", in Proc. 24th Eur. Photovoltaic Solar Energy conf., 891-895 (2009).

[10] A. Edler, V. Mihailetchi, R. Kopecek, R. Harney, T. Böscke, D. Stichenoth et al., "Improving screen printed metallization for large area industrial solar cells based on n-type material", Energy Procedia 8, 493-497 (2011).

[11] L.J. Geerligs, I.G. Romijn, A.R. Burgers, N. Guillevin, A.W. Weeber, J.H. Bultman et al., "Progress in low-cost n-type silicon solar cell technology", Proceedings of the 38th IEEE Photovoltaics Specialists Conference, 001701-001704, Petten, Netherlands, 2012.

[12] T.S. Böscke, D. Kania, A. Helbig, C. Schöllhorn, M. Dupke, P. Sadler et al., "Bificial n-Type Cells With >20 % Front-Side Effciency for Industrial Production", IEEE Journal of Photovoltaics 3 (2), 674-677 (2013).

[13] K. Bothe, R. Sinton, and J. Schmidt, "Fundamental Boron-Oxygen-related Carrier Lifetime Limit in Mono- and Multicrystalline Silicon", Prog. Photovolt: Res. Appl. 13, 287-296 (2005).

[14] J. Schmidt and A. Cuevas, **"**Electronic properties of light-induced recombination centers in boron-doped Czochralski silicon", J. Appl. Phys. 86 (6), 3175-3180 (1999).

[15] S. Rein and S.W. Glunz, "Electronic properties of metastable defect in boron-doped Czochralski silicon: Unambigous determination by advanced lifetime spectroscopy", Appl. Phys. Lett. 82 (7), 1054-1056 (2003).

[16] J. Schmidt, B. Lim, D. Walter, K. Bothe, S. Gatz, T. Dullweber, and P. Altermatt, **"**Impurity-related Limitations of Next-Generation Industrial Silicon Solar Cells", IEEE J. Photovolt. 99, 1-5 (2012).

[17] D. Macdonald and A. Cuevas, "Reduced Fill Factors IN Multicrystalline Silicon Solar Cells Due to Injection-level Dependent Bulk Recombination Lifetimes", Prog. Photovolt: Res. Appl. 8 (4), 363-375 (2000).

[18] R. Bock, J. Schmidt, R. Brendel, H. Schuhmann, and M. Seibt, **"**Electron microscopy analysis of crystalline silicon islands formed on screen-printed aluminum-doped p-type silicon surfaces", J. Appl. Phys. 104 (4), 043701 (2008).

[19] P.P. Altermatt, S. Steingrube, Y. Yang, C. Sprodowski, T. Dezhdar, S. Koc et al., „Highly predictive modeling of entire Si solar cells for industrial applications", in Proc. 24th Eur. Photovoltaic Solar Energy conf., 901-906 (2009).

[20] J. Müller, K. Bothe, S. Gatz, and R. Brendel, "Modelling the formation of local highly aluminum-doped silicon regions by rapid thermal annealing of screen-printed aluminum", Phys. Status Solidi RRL 6 (3), 111-113 (2012).

[21] J. Müller, K. Bothe, S. Gatz, H. Plagwitz, G. Schubert, and R. Brendel, "Contact Formation and Recombination at Screen-Printed Local Aluminum-Alloyed Silicon Solar Cell Base Contacts", IEEE Transactions on Electron Devices 58 (10), 3239-3245 (2011).

[22] T. Dullweber, S. Gatz, H. Hannebauer, T. Falcon, R. Hesse, J. Schmidt, and R. Brendel, **"**Towards 20% efficient large-area screen-printed rear-passivated silicon solar cells", Prog. Photovolt: Res. Appl. 20 (6), 630-638 (2011).

[23] S. Gatz, T. Dullweber, and R. Brendel, **"**Evaluation of Series Resistance Losses in Screen-Printed Solar Cells with Local Rear Contacts", IEEE J. Photovolt. 1 (1), 37-42 (2011).

[24] B. Hoex, J. Schmidt, R. Bock, P.P. Altermatt, M.C.M. van de Sanden, and W.M.M. Kessels, "Excellent passivation of highly doped p-type Si surfaces by the negative-charge-dielectric Al_2O_3", Appl. Phys. Lett. 91, 112107 (2007).

[25] B. Veith, F. Werner, D. Zielke, R. Brendel, and J. Schmidt, **"**Comparison of the thermal stability of single Al_2O_3 layers and Al_2O_3/SiNx stacks for the surface passivation of silicon", Energy Procedia 8, 307-312 (2011).